Journal of Bioenergetics and Biomembranes, Vol. 17, No. 5, 1985

"Exchange Diffusion": Rate Equations for the Influx of α-Aminoisobutyric Acid into Mouse Cerebrum Slices Containing This Amino Acid[1]

Stephen R. Cohen[2]

Received January 22, 1985; revised June 21, 1985

Abstract

Rate equations for the gross influx of α-aminoisobutyric acid (AIB) into mouse cerebrum slices containing AIB have a first-order term for unsaturable concentrative influx, identical to the corresponding term for unloaded slices, and a modified Michaelis–Menten term, $V'_{max}/(1 + K_t/S)$, for saturable concentrative influx. [$V'_{max} \equiv v'_L(1 + K_t/S)$, where v'_L = saturable component of influx, S = AIB concentration in medium, and K_t = Michaelis constant for unloaded slices.] Below a tissue AIB (T) of 19 μmol/g final wet weight, V'_{max} increases linearly following $V'_{max} = V_1 + m_1 T$; above that value, V_{max} is virtually constant. The transition is sharp. This equation is consistent with a carrier model for active transport. At the transition, intracellular AIB is about 1 molecule for every 70 amino acid residues of tissue protein, vastly more than could be accommodated by AIB-binding sites in cell membranes. The transition may come from a slow process that does not fill all sites when the tissue AIB is below the transition concentration, or from an AIB-induced phase transition in the membrane.

Key words: α-Aminoisobutyric acid; amino acids; brain slices; exchange diffusion; kinetics; membrane transitions; rate equations; transport.

Introduction

Active biological transport and mediated biological transport frequently show "exchange diffusion"; that is, gross flux is stimulated by the presence of the transport substrate or a related subsance on the opposite side of the cell membrane. This increased flow is accompanied by counterflow of the substance that elicits this effect. "Exchange diffusion" of ions has been known for

[1] For my wife, Lynn.

[2] New York State Office of Mental Retardation and Developmental Disabilities, Institute for Basic Research in Developmental Disabilities, 1050 Forest Hill Road, Staten Island, N.Y. 10314.

0145-479X/85/1000-0305$04.50/0

at least 35 years (Ussing, 1949), and "exchange diffusion" of molecules for at least 30 (Heinz, 1954). This effect (which is not a diffusive process) is found in systems ranging from single cells to complex tissues. Its existence appears to be paradoxical because it works against the regulation of the supply of metabolite to cells or the control of the tissue level of a substance by transport. "Exchange diffusion" is predicted by models of carrier-mediated transport if certain relations hold among the rate constants of the individual steps (Eilam and Stein, 1974; Hoare, 1972; Lieb and Stein, 1974). [See the elegant summary of transport kinetics by Stein (1981).] These relations need not occur; transport without "exchange diffusion" is known. Kinetic analyses reveal no function for "exchange diffusion". It may be a consequence of the necessity for building pumps from proteins and phospholipids instead of stainless steel and silicone elastomers.

Reliable quantitative studies of the kinetics of "exchange diffusion" in preparations of tissues with a complex structure and with interactions among cells are scarce. The present study was undertaken to establish empirical rate equations for "exchange diffusion" in such a tissue, using as a model system the influx of the synthetic amino acid AIB (see the Nomenclature section for abbreviations) into incubated mouse cerebrum slices preloaded with AIB. The kinetics of AIB uptake by brain slices incubated under various conditions in several media have been determined (Cohen, 1973*a*, 1980*a*, 1980*b*, 1981, 1985).

Materials and Methods

Gross Influx

Gross influx was determined by measuring the uptake of ^{14}C-labeled AIB that was added to the medium after the slices had been loaded with unlabeled AIB. In *constant-concentration* runs, the concentration of AIB in the medium was not changed by the addition of labeled substrate. In *concentration-profile* runs, the concentration was increased.

With minor changes the procedures were those used in earlier studies of influx kinetics (Cohen, 1973*a*, 1975, 1980*a*, 1980*b*, 1981, 1985). Six- to nine-week old male, white Swiss mice, strain CF-1, were decapitated and the brain rapidly removed. Olfactory bulbs and underlying white matter were trimmed from the cerebral hemispheres, which were then immersed for a few seconds in chilled, substrate-free medium. The hemispheres were taken from the medium, blotted, and cut into nominally 0.416 mm-thick slices, as described by Blasberg and Lajtha (1965) using a calibrated (Cohen, 1974) McIlwain–Buddle (1953) tissue chopper. Slices from one hemisphere (about 125–150 mg) were placed in a stoppered 25-ml erlenmeyer flask containing 4.5 ml of

oxygenated medium at 37° C with unlabeled AIB at a preselected concentration from 0.2 to 20 mM. To load tissue, slices were incubated at bath temperature with gentle shaking for 30 min in a thermostatted reciprocating water-bath shaker. A 0.5-ml portion of medium at 37° C containing [1-^{14}C]AIB was added quickly and incubation continued for a predetermined time. The slices were then rapidly filtered off with suction. The resulting tissue pellet was frozen in solid CO_2 for ease of handling, weighed, homogenized in 2 ml of 5% (wt./wt.) perchloric acid, centrifuged, and the concentration of labeled AIB in the supernatant determined by liquid scintillation counting of a 0.5-ml aliquot as described previously (Cohen, 1985). These counts were compared to the average activity of 0.5-ml aliquots of three references, each prepared by adding to 2 ml of perchloric acid 100 μl of the solution of [1-^{14}C]AIB that was added to the incubation medium. Quench corrections were unnecessary because tissue extracts and references had the same counting efficiency. Counts per gram of tissue is $G = (4 + 1.6w)C/w$ (Cohen *et al.*, 1968). The equivalent activity of the reference is $A = 4.2C_R$. The uptake of AIB relative to medium (in percent tissue space) is $U_R = 100G/A$. The absolute uptake (in μmol AIB/g final wet weight of tissue) is $U = U_R S/100$. A graph of U_R as a function of the incubation period was drawn for each run. Each graph had a pronounced linear region, usually from 2 to 7 min. Gross influx is the concentration of AIB in the medium times the slope of this region. The slope was calculated by least squares on y from uptake for at least five incubation periods, each run in triplicate. This procedure eliminates the contribution of labeled AIB on the surface of the slices and in the *functional* extracellular space for AIB uptake, a tissue compartment that cannot be measured at present (Cohen, 1972). Because the labeled AIB is diluted by the unlabeled AIB in the loaded tissue, a negligible fraction of the counts is lost through efflux, and therefore the measured rate is effectively the rate of initial gross influx. The counts are a true measure of [^{14}C]AIB because AIB is not metabolized.

AIB in Loaded Tissue

To measure total tissue AIB, slices, prepared as above, were incubated at 37° C with shaking for 25, 30, 35, 40, 45, or 50 min in 5 ml of oxygenated medium containing 0.2 to 20 mM [1-^{14}C]AIB, then filtered off and counted as above. Each point was determined in triplicate. Triplicate references were prepared as above from the incubation medium. In these runs $A = 42C_R$. The AIB content of tissue incubated for 30 min was calculated from equations that were fitted separately to the data for each concentration in the medium. From these values the empirical relation

$$T = 11S/(1.88 + S) + 1.33S \qquad (1)$$

for the AIB content of slices incubated for 30 min was found by curve fitting. (Details will be published separately; Cohen, in preparation.) Intracellular concentrations were calculated using the formula

$$T_i^w = (T - W_e S/100)/(1 - W_d - W_e/100) \quad (2)$$

taking the dry weight of slices incubated for 30 min to be 0.161 g/g final wet weight (Cohen *et al.*, 1970) and assuming the extracellular space to be 20, 25, or 30% by weight.

Incubation Medium

HEPES-buffered medium (Cohen *et al.*, 1970) with added AIB was used. Standard medium without AIB contains (in mM): NaCl 119; KCl 5.0; $CaCl_2$ 0.75; $MgSO_4$ 1.2; NaH_2PO_4 1.0; $NaHCO_3$ 1.0; HEPES 25; NaOH 12, which reacts to form the complementary base of the buffer; and glucose 10. It has a nominal tonicity of 300 milliosmoles and a pH of 7.2 at 37° C.

Reagents

[1-^{14}C]AIB was from New England Nuclear (Boston, Massachusetts). Unlabeled AIB and HEPES were from Sigma Chemcial Co. (St. Louis, Missouri). Other chemicals were ACS or reagent grade from various sources.

Curve Fitting and Comparative Fit

Equations (5) and (6) were fitted by least squares y with V'_{max} as the dependent variable. The relative error of the fit of V'_{max} (Table I) was calculated with $P = 2$, and with $n = 10$ in Region 1, and 3 in Region 2. The nonlinear forms of Eqs. (9)–(13) with different values of the exponents were fitted directly to data. By definition, the minimum of the sum of the squares of the relative deviations of Δv, that is, the minimum value of $\Sigma[(\Delta v_{obs} - \Delta v_{calc})/\Delta v_{calc}]^2$, gave the best fit (see Cohen, 1968). The rate equations were compared for their fit to constant concentration data and to concentration profile data by calculating the relative error of v_L. Because the exponents were fixed before fitting Eqs. (9)–(13), $P = 2$ for Eqs. (7)–(10), and 3 for Eqs. (11)–(13). (The constant-composition run with $S = 10$ mM was not used to fit equations.) To minimize round-off errors in calculated rates, fitted parameters are reported to more figures than are warranted. Additional figures are kept in Table I and elsewhere to show small differences, and especially differences between fits with the substrate in tissue expressed as T, T_i^{20}, T_i^{25}, or T_i^{30}. The precision of the several kinetic parameters was not estimated because the kinetic parameters are not linearly independent, and because they were calculated using assumed values for K_t and k_u. This

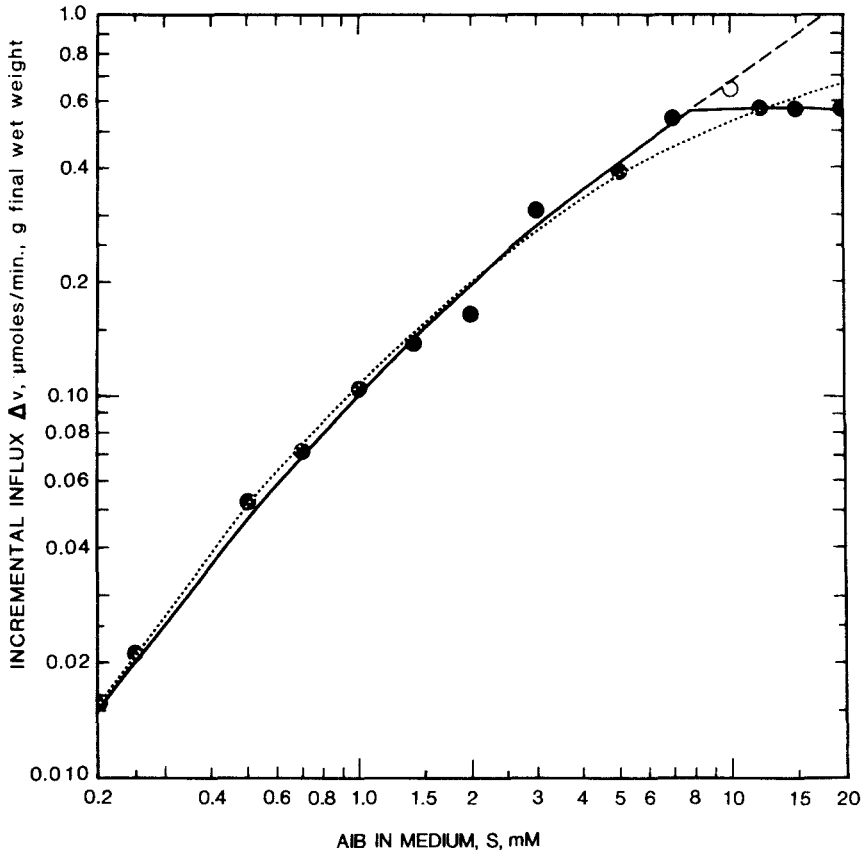

Fig. 1. Incremental influx, Δv, as a function of AIB in medium. All data are from constant-concentration runs. ●, Data point used for curve fitting. ○, Data point not used for curve fitting ($S = 10$). Solid curves are fitted curves [Eq. (5), Region 1, or (6) Region 2] calculated from values in Table I, column headed T, and from kinetic parameters for influx into unloaded slices [$V_{max} = 0.404$ μmol AIB/min, g final wet weight; $K_t = 1.115$ mM (Cohen, 1985)]. Dashed curve is extension of Eq. (5) in Region 2. Dotted curve is fitted curve [Eq. (15)] for Δv over entire range $S = 0.2$ to 20 mM.

statistic is not necessary for the purposes of this study. The fit of rate expressions to data is consistent with the fit in our earlier studies (see the Results section, Agreement with Concentration-Profile Data).

Results

The incremental gross influx Δv of AIB in constant-composition runs falls on two curves that intersect close to $S = 8$ mM (Fig. 1). At lower concentrations (Region 1), Δv increases with S. At higher concentrations

(Region 2) Δv is essentially constant at about 0.57 μmol AIB/min, g final wet weight. Although Δv is presented as a function of S, influx is also dependent on the concentration of AIB in the tissue.

Rate Equations for Gross Influx: The Apparent V_{max}

As T approaches zero, the equation for gross influx should reduce to the rate equation for unloaded tissue. The rate equation for the uptake of AIB, GABA, *L*-leucine, and *L*-lysine by unloaded brain slices is

$$v = V_{max}S/(K_t + S) + k_uS \tag{3}$$

This has two *kinetically* independent terms: $V_{max}S/(K_t + S)$ representing saturable Michaelis–Menten influx, and k_uS representing unsaturable, first-order influx (Cohen, 1973*a*, 1975). For the uptake of AIB from the glucose medium used in these studies V_{max} is 0.404 μmol/min, g final wet weight, K_t is 1.115 mM, and k_u is 0.0528 μmol/min, mM amino acid in medium, g final wet weight (Cohen, 1975, 1985). Presumably a similar two-term equation describes gross influx in slices containing AIB.

At AIB concentrations in the medium that correspond to Region 2, the unsaturable component is the major pathway for AIB uptake by unloaded slices, providing 63% of influx when S is 12 mM and 73% when S is 20 mM (Cohen, 1975). It is highly unlikely that any large differences between unsaturated influx in loaded and unloaded slices would be so nicely compensated by differences in unsaturable influx as to keep Δv nearly constant in this region. Therefore the unsaturable component was assumed to be unchanged by tissue AIB. Using the value of k_u for unloaded slices, this component, k_uS, was subtracted from measured rates for loaded slices. This difference was taken to be v'_L, the saturable component of influx.

The *apparent maximum rate* of saturable transport, defined by

$$V'_{max} \equiv v'_L(1 + K'_t/S) \tag{4}$$

was calculated for both regions assuming K'_t to be equal to K_t for unloaded slices. This expression is the Michaelis–Menten equation solved for V_{max} with the essential difference that V'_{max} is a function of the quantities v'_L and S, and the parameter K'_t. Figure 2 shows V'_{max} as a function of T. The graph consists of two intersecting straight lines. (This linear relation justifies setting K'_t equal to K_t.) In Region 1, V'_{max} increases strongly with T according to the relation

$$V'_{max1} = V_1 + m_1T \tag{5}$$

In Region 2, V'_{max} decreases slightly with increasing T according to the relation

$$V'_{max2} = V_2 + m_2T \tag{6}$$

Table I. Numerical Values for the Equation $V'_{max} = V + mT$ [Eqs. (5) and (6)] and the Transition Point Between Regions 1 and 2[a]

Quantity	Measure of tissue AIB			
	T	T_i^{20}	T_i^{25}	T_i^{30}
Region 1				
V_1	0.466	0.461	0.460	0.458
m_1	0.03000	0.02081	0.01959	0.01833
r	0.988	0.987	0.987	0.987
$(V_1 - V_{max})/V_{max}$, %	15.3	14.1	13.7	13.3
Relative error, %	3.7	3.9	3.9	3.9
Region 2				
V_2	1.094	1.097	1.099	1.100
$m_2 \times 10^3$	−2.61	−1.94	−1.87	−1.79
r	−0.984	−0.984	−0.984	−0.984
Relative error, %	0.4	0.4	0.4	0.4
Transition				
T or T_i^w	19.24	27.91	29.77	31.90
T_{int}	19.24	19.47	19.53	19.60
S_{int}	7.80	7.95	7.99	8.04
V'_{int}	1.043	1.043	1.043	1.043

[a] Units: S, mM AIB; T, μmol AIB/g final wet weight of tissue; T_i^w, μmol AIB/g intracellular water assuming w percent extracellular water; V, μmol AIB/min, g final wet weight; m μmol AIB/μmol tissue AIB, min, or [μmol AIB/(μmol tissue AIB, min)] × (g intracellular water/g final wet weight).

The corresponding rate equations for the gross influx are

$$v_L = (V_1 + m_1 T)/(1 + K_t/S) + k_u S \tag{7}$$

in Region 1, and

$$v_L = (V_2 + m_2 T)/(1 + K_t/S) + k_u S \tag{8}$$

in Region 2.

Fits to Measures of Intracellular AIB. Preferably the rate equations should show the dependence on the intracellular concentration, not on T, which is a weighted average of the intracellular and extracellular concentrations. Graphs were constructed of V'_{max} as a function of intracellular AIB assuming 20, 25, or 30% extracellular water. With these three measures, as with T, the data define two intersecting straight lines. (Compare Fig. 3, the graph for T_i^{30}, with Fig. 2.) Although an exact linear dependence on any one requires a nonlinear dependence on the others, the curvature is slight and is completely obscured by experimental scatter. Table I contains the constants for rate equations in each region, the coordinates of the intersection, and measures of the goodness of fit of these rate expressions. The fit is the same for all four measures of tissue AIB. The intercepts V_1 and V_2, and the intersection point are almost independent of the measure of tissue AIB.

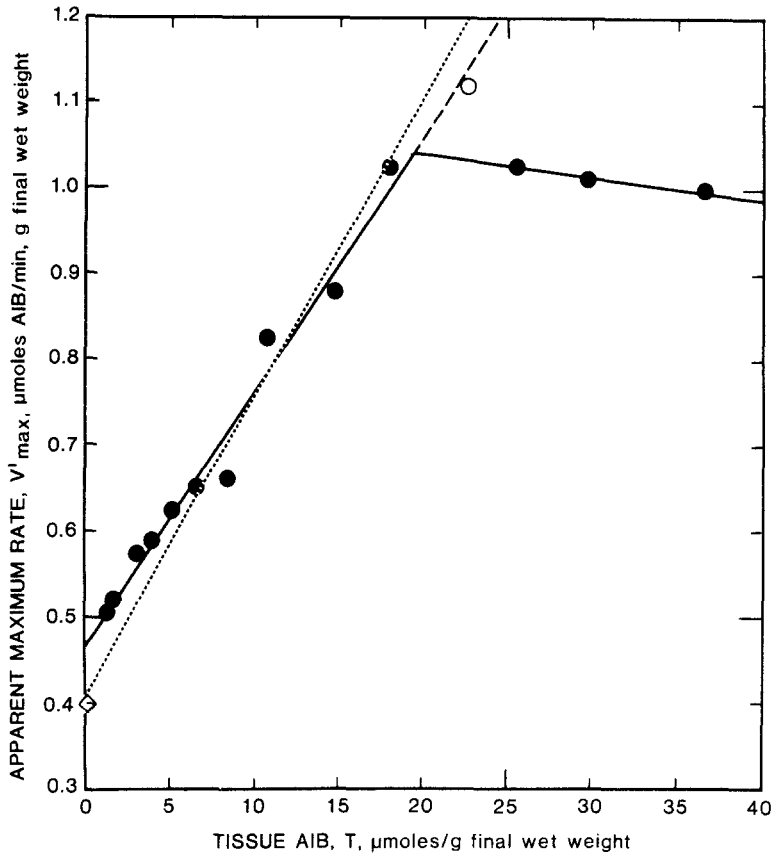

Fig. 2. Apparent maximum rate, V'_{max}, as a function of AIB in tissue. All data are from constant-concentration runs. ●, Data points used for curve fitting. ○, Data point not used for curve fitting ($S = 10$). ◇, V_{max} for uptake by unloaded slices. Solid curves are fitted curves [Eq. (5), Region 1, or (6), Region 2] were calculated from values in Table I, column headed T. Dashed curves is extension of Eq. (5) in Region 2. Dotted curve is linear equation for V'_{max} fitted to data in Region 1 with the intercept $V_1 = V_{max}$ for unloaded slices, by definition.

Going from T to T_i^{30}, S_{int}, the value of S corresponding to the tissue AIB at the intersection, is increased by 3%. Other quantities are affected less. Therefore in the present instance, and presumably in many others, the concentration in tissue, which is measurable, can be freely substituted for the unmeasurable true intracellular concentration with little distortion. This is a great convenience.

In all further analyses of the data, T is used as the sole measure of AIB in the slices.

Agreement with Concentration-Profile Data. The expected gross influx in concentration-profile runs, calculated from Eqs. (7) and (8), was compared with data. Figure 4 presents profiles for tissue loaded with 2 and 5 mM AIB,

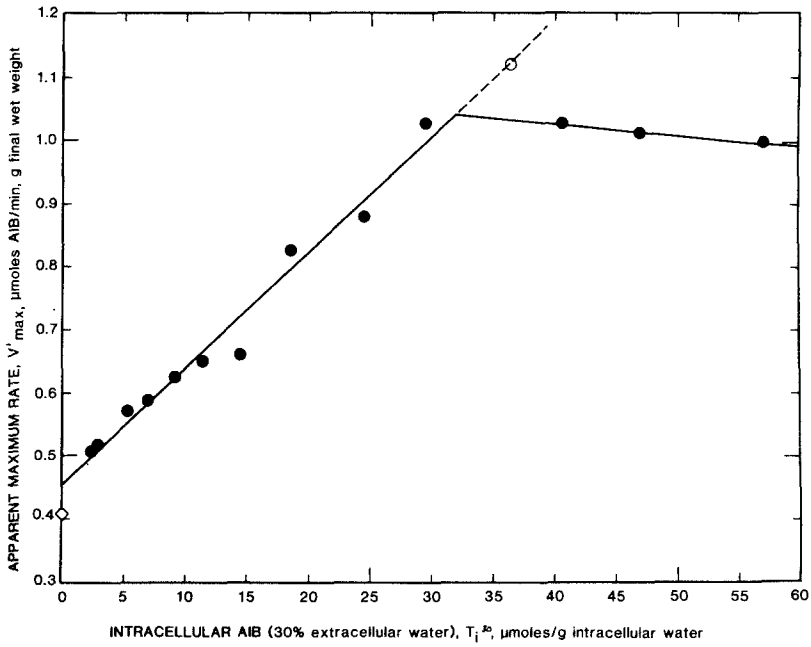

Fig. 3. Apparent maximum rate, V'_{max}, as a function of intracellular AIB. All data are from constant-concentration runs. Extracellular and surface water was assumed to be 30% of weight of incubated slice. Dry weight is 0.161 g/g final wet weight (Cohen *et al.*, 1970). ●, Data point used for curve fitting. ○, Data point not used for curve fitting (S = 10 mM). ◇, V_{max} for uptake by unloaded slices. Solid curves are fitted curves [Eq. (5), Region 1, or (6). Region 2] calculated from values in Table I, column headed T_i^{30}. Dashed curve is extension of Eq. (5) in Region 2.

and gross uptake of 20 mM AIB by slices loaded with 0.2, 0.5, 10, and 15 mM AIB. Excluding the constant-concentration run at the start of each profile there are 10 values in Region 1 to test the rate equation. There is a very severe test, because none of these data points were used to develop this equation or to evaluate its parameters. The relative error of v_L is 8.5%, which is consistent with the agreement between measured and computed rates in our other studies of amino acid uptake by brain slices (Cohen, 1975, 1980*b*, 1981, 1985). (If the initial constant-concentration runs are included, the relative error is 7.3%. If all runs are considered, it is 6.0%.) There is no systematic divergence of the observed from the calculated rates. This agreement strongly supports rate equation (7) for Region 1. If the AIB content of the loaded slices lies in Region 1, Eq. (7) applies even when the final AIB concentration in the medium lies in Region 2. If it lies in Region 2, Eq. (8) for Region 2 applies.

Influx of 20 mM AIB into slices loaded with 15 mM substrate fits Eq. (8), as might be expected. The measured rate is 1.5% below the rate calculated from this equation and is 16% below the rate calculated from Eq. (7).

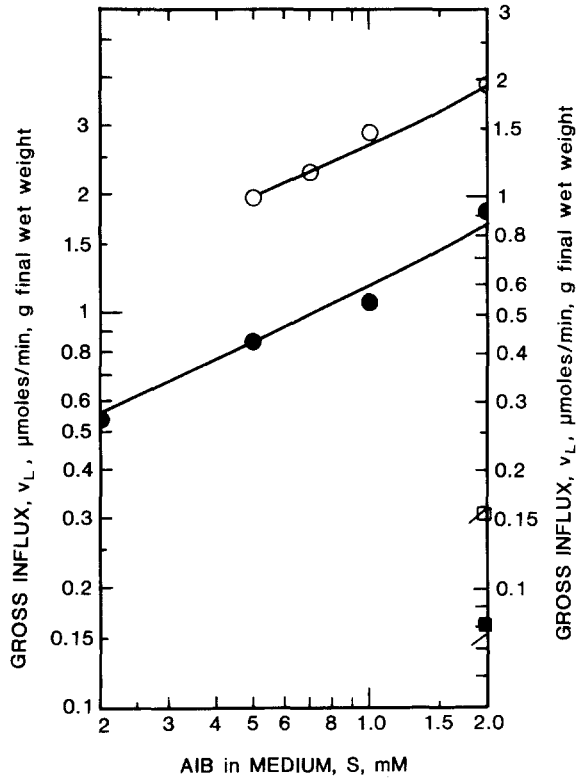

Fig. 4. Concentration-profile data for gross influx as a function of AIB in medium during uptake. ○, Slices loaded with 5 mM AIB (right-hand scale). ●, Slices loaded with 2 mM AIB (left-hand scale). □, Slices loaded with 0.5 mM AIB (right-hand scale; multiply value by 10). ■, Slices loaded with 0.2 mM AIB (left-hand scale; multiply value by 10). Lines were calculated from Eq. (7) using values in Table I, column headed T, and kinetic parameters for influx into unloaded slices [V_{max} = 0.404 μmol AIB/min, g final wet weight; K_t = 1.115 mM; k_u = 0.0528 μmol AIB/min, g final wet weight, mM AIB in medium (Cohen, 1985)].

It is not clear which equation applies to slices loaded with 10 mM AIB. The constant-concentration data point lies on the extrapolated curve for Region 1 even though the tissue AIB is greater than the intersection value (Figs. 1–3). This rate, 1.535 μmol/min, g final wet weight, is 1.4% less than the calculated rate for Region 1 and 5.2% greater than the calculated rate for Region 2. The observed gross influx of 20 mM AIB in the concentration-profile run is closer to the expected value for Region 2 (Fig. 4). This rate, 1.965 μmol/min, g final wet weight, is 8.1% less than the calculated rate for Region 1, but only 3.5% less than the calculated rate for Region 2. Because values from Eqs. (7) and (8) differ little near the transition, it is difficult to

make measurements with sufficient precision to clearly reveal overshoot or hysteresis near the transition.

The Discrepancy between V_1 and V_{max}. Although V_1, the limiting value of V'_{max} at infinitesimal AIB loading, should equal V_{max}, it is 13–15% greater (Table I). To test whether this discrepancy comes from random error, V_1 was set equal to V_{max} by *fiat* and the linear equation $V'_{max} = 0.404 + 0.03552T$, with units of V'_{max}, μmol AIB/min g final wet weight, obtained by a least-squares fit on y to the constant-concentration measurements in Region 1 (compare with values in Table I). The fit is appreciably poorer. The relative deviation of V'_{max} is increased from 3.7 to 8.5%. More significantly, the fitted line differs systematically from calculated values (Fig. 2), showing that the difference is not due to random error.

In Region 2, the decrease of V'_{max} with increasing T may show some slight effect of tissue AIB on the unsaturable component, contrary to the assumption used to develop equations for gross influx. Three modified expressions for the unsaturable component were tested, largely to ascertain whether this assumption contributes to the discrepancy between V_1 and V_{max}. They are: (a) $k_u S - \alpha T$, (b) $k_u S(1 - \beta T)$, and (c) $k_u S/(1 + \gamma T)$. Modified values (V''_{max}) for V'_{max} were calculated using $V''_{max} = (v_L - \text{modified unsaturable uptake})(1 + K_t/S)$ with α, β, or γ chosen to make the slope of a line fitted to V''_{max} in Region 2 zero with K_t and k_u assuming their values for unloaded slices. Modifications (b) and (c) have little effect on V_1 or V'_{int}; modification (a) increases both these quantities. Therefore it is unlikely that this discrepancy is an artifact arising from assuming the unsaturable component to be independent of tissue AIB. (See the Discussion for a possible source of this discrepancy.)

Rate Equations for the Incremental Influx: Expressions for Δv

An excellent fit of one empirical equation does not preclude others. The following extensions of the Michaelis–Menten equation were fitted to constant-concentration measurements of incremental influx:

$$\Delta v(T^\tau) = U_{max}/(1 + K/T^\tau) \tag{9}$$

$$\Delta v(S^\sigma T^\tau) = U_{max}/(1 + K/S^\sigma T^\tau)$$

$$= U_{max}/(S + K/S^{\sigma-1} T^\tau) \tag{10}$$

$$\Delta v(T^\alpha, T^\beta) = U_{max}/(1 + K_\alpha/T^\alpha + K_\beta/T^\beta) \tag{11}$$

$$\Delta v(S^\alpha, T^\tau) = U_{max}/(1 + K_\sigma/S^\sigma + K_\tau/T^\tau) \tag{12}$$

$$\Delta v(S^\sigma, ST^\tau) = U_{max}/(1 + K_\sigma/S^\sigma + K_\tau/ST^\tau)$$

$$= U_{max} S/(S + K_\sigma/S^{\sigma-1} + K_\tau/T^\tau) \tag{13}$$

where U_{max} corresponds to the Michaelis–Menten V_{max}, and the K's to Michaelis constants. All ensure that the rate equation will agree with the equation for unloaded slices when $T = 0$, that Δv will approach an upper limit in agreement with observations (Fig. 1), and that the parameters can be assigned some physical meaning. (Power series and other empirical expressions with meaningless parameters were not considered.) Similar generalizations of the Michaelis–Menten equation have been derived from models for complex enzyme kinetics and for carrier transport. [See, for example, Vidaver and Shepherd (1969).] Analogous expressions cannot be considered for gross influx because, for all values of S, $v_L' = 0$ when $T = 0$. Processes with complex kinetics may have nonintegral or variable-order rate equations (Benson, 1960). Therefore integral and half-integral exponents were assumed. Exponents ranged from 1/2 to 2 except in Eqs. (10) and (13) where integral and half-integral values of σ ranged from 1 to 3. Negative exponents or higher exponents are hard to justify physically. Because negative parameters are meaningless, the relative error in Δv was calculated only for those sets of exponents that gave positive parameters when fitted to data for Region 1, and for Regions 1 and 2 combined (excluding the value at $S = 10\,\text{mM}$).

Twenty-eight met this requirement. Of these, seven fitted to Region 1 data have a relative error in Δv in this region no more than 20% greater than the relative error in Δv calculated from Eq. (5). None have less relative error. In Region 1 these eight equations give virtually identical graphs of Δv versus S.[3] All fail in Region 2, the computed rate becoming increasingly greater than the measured rate as S increases. When tested against the concentration-profile measurements in Region 1, all were eliminated except Eq. (13) with $\sigma = 1$ and $\tau = 3/2$, that is,

$$v = U_{max}/(1 + K_\sigma/S + K_\tau/T^{3/2}) \tag{14}$$

where $U_{max} = 1.898\,\mu\text{mol/min, g final wet weight}$, $K_\sigma = 6.50\,\text{mM}$, and $K_\tau = 129.1\ (\mu\text{mol/g final wet weight})^{3/2}$, which has a relative error of v_L that is only 10% greater than the error of Eq. (7). Statistically these two very different equations, (5) and (14), are equally valid empirically expressions for uptake in Region 1.

All best fits of Eqs. (9)–(13) to the complete range of constant-concentration data are distinctly poorer. The best, when tested against concentration-profile measurements, is

[3] These trial fits illustrate the principle that agreement of an equation with data does not establish the validity of the equation except as a computational device until other plausible equations have been ruled out.

$$v = U_{max}/(1 + K_\sigma/S + K_\tau/T^2) \quad (15)$$

where $U_{max} = 0.840\,\mu$mol/min, g final wet weight, $K_\sigma = 4.90$ mM, and $K_\tau = 51.2$ (μmol/g final wet weight)^2. Although the *best*, it fails near the transition and in Region 2 (Fig. 1). Several others give graphs of Δv versus S over the range $S = 0.2$ to 5 mM that are nearly identical to the graphs of the eight equations discussed above; however they all have a pronounced positive slope in Region 2 and a gradual curve in the transition region. With the assumed restrictions on exponents and parameters, no set gives a graph of Δv versus S that conforms to the data (see Fig. 1) by showing a gently curved, steadily increasing function in Region 1, by being nearly flat in Region 2, and by having a sharply rounded knee at the transition. If fitted to data for higher concentrations, rather than the complete set of data, the curve for lower concentrations is too steep, and either underestimates Δv at all lower concentrations–the relative error becoming more serious as S decreases–or balloons out, overestimating Δv at intermediate concentrations, for example $S = 0.5$ to 5 mM, while still underestimating Δv at the low end. Even if statistical criteria are jettisoned, the exponents and parameters cannot be adjusted to produce a sharp knee. Because these equations embrace a wide variety of physically interpretable rate equations, it is unlikely that other physically meaningful expressions can do so. Therefore the observed break is not an artifact of data treatment.

Discussion

Comparison with the Literature

Published studies contain few indications of the findings reported here. Equation (7) predicts that at a fixed substrate concentration in the medium, gross influx will be a linear function of substrate in the tissue. This was observed by Heinz and Walsh (1958, Fig. 3, this reference) for the uptake of glycine by Ehrlich ascites cells.

If synthesis or metabolic loss contribute little, gross efflux approximates gross influx at steady state. Miller's (1968) data for the efflux of glucose from red cells at equilibrium [see Lieb and Stein (1970), Fig. 5, this reference], and Cabantchik and Ginsburg's (1977) data for the efflux of uridine from red cells at equilibrium (see Fig. 3, this reference) can be interpreted as lying on two curves with a transition, although the authors do not do so. The transition for glucose is at an intracellular concentration of about 50 mM; that for uridine is at about 3 mM. Both are within an order of magnitude of the intracellular concentration at the intersection (Table I).

Theory of Carrier-Mediated Transport

Carrier-mediated transport is capable of "exchange diffusion" if free carriers exist in two interconvertible forms, one for influx and one for efflux. If transport is through "pores", or if free carriers exist in one form that serves indifferently for both influx and efflux, intracellular substrate, by competing for the "pores" or carriers, can only be reduce influx. Consider the following schematic mechanism for influx:

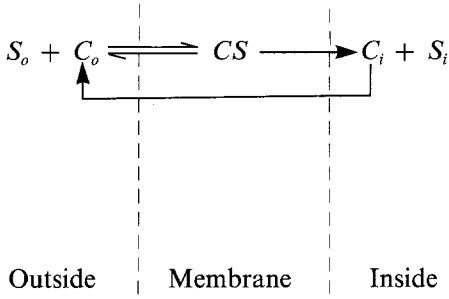

In this model the substrate, S, crosses the membrane as a complex, CS, with a carrier, C, that can exist in the membrane in two free forms: C_o, which reacts reversibly with S_o, substrate outside the cell, to form CS; and C_i, which reacts reversibly with S_i, substrate inside the cell, to form CS. Once formed, CS either reverts to C_o and S_o or releases substrate inside the cell, leaving C in the form C_i which is then converted to C_o to continue the process. The reverse process produces efflux. If there is substrate on both sides, influx and efflux occur simultaneously. If the reaction $C_i + S_i \rightarrow CS \rightarrow C_o + S_o$ is faster than the reaction $C_i \rightarrow C_o$, efflux through this system, by decreasing its turnaround time, increases the effective capacity of the carrier, and the system exhibits "exchange diffusion". If it is slower, the reverse flow decreases influx. Assuming the usual steady-state approximation, this mechanism gives the rate equation for influx

$$v_L = V_{\max}(1 + \mu T_i)S/(K_t + S + PT_i + QST_i) \tag{16}$$

where $V_{\max}$, μ, K_t, P, and Q are functions of the rate constants for the individual steps (Stein, 1981).[4] (The phenomenological kinetics are the same if the complex exists in two interconvertible forms, $(CS)_o$ and $(CS)_i$, at the outer and inner surface of the membrane. Any scheme that requires two

[4]This is Stein's (1981) equation (30) for carrier-mediated influx, slightly rearranged, with these substitutions for Stein's notation: $v = f_{12}$, $S = S_1$, $T_i = S_2$, $V_{\max} = 1/R_{12}$, $\mu = 1/K$, $K_t = KR_{00}/R_{12}$, $P = R_{21}/R_{12}$, and $Q = R_{ee}/R_{12}K$. Although here Stein considers only mediated transport, this equation describes active transport (Eilam and Stein, 1974) if the carrier system is assumed to be coupled to an energy source.

separate but interconvertible forms of the carrier and is consistent with the above mechanism will give the same rate equation.) The general condition for "exchange diffusion" is $\mu > (P + QS)/(K_t + S)$. (Here V_{max} and K_t have the same meaning as in other equations.) This can be solved for $V'_{max} = v_L(1 + K_t/S)$ to get

$$V'_{max} = V_{max}(1 + \mu T_i) \times [(K_t + S)/(K_t + S + PT_i + QST_i)] \quad (17)$$

In this equation V'_{max} is the linear expression $V_{max}(1 + \mu T_i)$ multiplied by the factor in square brackets. This factor is always less than 1. If PT_i and QST_i are negligible compared to K_t, this factor approaches 1 and

$$V'_{max} = V_{max}(1 + \mu T_i) \quad (18)$$

This is Eq. (5) with $V_1 = V_{max}$ and $m_1 = \mu V_{max}$. This factor decreases as both S and T_i increase, as in a series of constant-concentration runs, and therefore, if V'_{max} is found from constant-concentration measurements, a graph of V'_{max} as a function of T_i (or of T) will be convex (Fig. 5). If random error obscures the curvature, the data will appear to fit a straight line with the intercept $V_1 > V_{max}$ (Fig. 5). The observed difference between V_1 and V_{max} in Region 1 may be a consequence of representing the data by a linear approximation to Eq. (17).

Alternative Rate Expressions

The distinction between Eq. (5) for V'_{max} and Eq. (14) for Δv is fundamental. An expression for the *total gross influx* of the transport substrate into tissue loaded with this substrate or with an allied substrate implies that the additional influx is carried by one or more of the systems for influx into unloaded tissue; an expression for the *incremental influx* implies that this incremental influx comes from other systems. Because tissues are unlikely to have a transport system dedicated to "exchange diffusion", this incremental influx must be a secondary effect from a transport system serving some other purpose. This could be one of the systems supporting amino acid efflux, which are at least partially distinct from those for influx (Cohen, 1973*b*). The carrier model provides for counterflow even when the system does not exhibit the enhanced gross flux of "exchange diffusion". The incremental uptake by loaded slices may be counterflow accompanying efflux. Since such counterflow, although observed as "exchange diffusion", is not carried out by the influx systems, it is properly expressed as a function of S and T (or T_i) to be added to the rate equation for influx. This hypothesis says nothing about the form of this Δv term.

On nonstatistical grounds Eq. (5) for V'_{max} is much to be preferred over Eq. (14). Its functional form is consistent with the general rate equation (17)

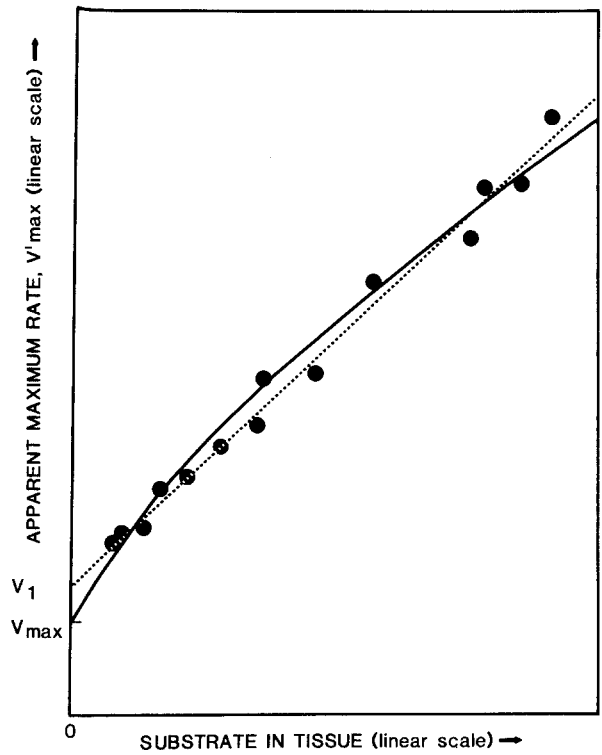

Fig. 5. Schematic diagram showing linear approximation to theoretical dependence of apparent maximum rate on substrate in tissue. Solid curve is theory, Eq. (18). Dotted curve is linear approximation. Note that curvature is obscured by experimental scatter. Note too that V_1, the intercept of the fitted linear approximation, is greater than V_{max}.

derived from the carrier model for active transport. One parameter, K_t, agrees with the value for unloaded slices, and to this extent it is not an empirical parameter to be fitted to observations. An analogous equation, (6), with the same value for K_t, fits the data in Region 2. The theoretical justification of equations for Δv does not favor a generalized Michaelis–Menten expression over other functional forms. Equation (12) has more adjustable quantities than Eq. (5), three parameters and two exponents compared with two constants, and therefore, in principle, can be more nicely fitted to data. Despite this, the fit is no better. The best exponent of T when it is fitted to data in the range $S = 0.2$ to 7 mM differs from the best exponent when it is fitted to data in the entire range 0.2–20 mM. The $T^{3/2}$ term in Eq. (14) is inconsistent with any obvious simple mechanism. In Region 2 the observed Δv decreases slightly, from 0.57 to 0.56 μmol/min, g final wet weight. If restricted to positive parameters and exponents, generalized Michaelis–Menten

equations cannot yield a decreasing Δv with increasing S or T, and will give a constant Δv only in the trivial limiting case of $\Delta v = U_{max}$.

The Transition

The observed break almost certainly represents some real reaction or process. It could not be reproduced by any of the trial rate expressions [Eqs. (9)–(13)]. Furthermore, the theoretical rate equations, (16) and (17), for carrier-mediated transport predict a gentle curve, not a knee.

Stoichiometry. Mouse-brain slices, incubated for 30 min, contain 16% dry weight (Cohen *et al.*, 1970); unsliced mouse brain contains 21% dry weight including 12% protein (Folch-Pi, 1955). At the intersection the slices contain somewhat over 19 μmol/g of AIB (Table I). If incubated tissue contains 30% extracellular water (a high estimate), then at the intersection it contains about 3 μmol of extracellular AIB and 16 μmol of intracellular AIB/g. (Less extracellular water would mean more intracellular AIB.) Assuming $12 \times (16\%/21\%) = 9\%$ protein in incubated slices, there is 1 molecule of intracellular AIB for every 5.7 kilodaltons of protein. The average molecular weight of the 20 amino acid residues found in proteins is 119. Assuming an average value of 100, there is 1 intracellular AIB molecule for every 57 residues. The average polypeptide subunit of a protein contains well over 100 residues; therefore, there is insufficient tissue protein to react with the intracellular AIB even assuming one binding site per subunit. The actual deficit is much larger because any reaction with AIB that alters transport must be restricted to specific membrane sites.

Chemical Equilibria. Assume that the intersection point represents the concentration of AIB needed in tissue to drive an equilibrium reaction with tissue to virtual completion. The binding must be weak, because a large excess of AIB is needed. Therefore except at low AIB concentrations there is little difference between the total tissue AIB and the free tissue AIB. Let A represent AIB; M represent a binding site; and K_d represent the dissociation constant for the A · M complex. Let P_1 be a property (say V_{max}) of uncomplexed tissue; P_2 be that property of complexed tissue; and P_{12}, the observed average property of the tissue. Assume the reversible reaction $A + M \rightleftharpoons A \cdot M$. At equilibrium

$$P_{12} = P_1 + (P_2 - P_1)[A]/([A] + K_d) \tag{19}$$

This is mathematically the same as the Michaelis–Menten equation with the added constant term P_1, and therefore, like the Michaelis–Menten plot, a graph of P_{12} as a function of free tissue AIB (or total tissue AIB) will be gently rounded. (If the general reversible reaction $aA + mM \rightleftharpoons A_a \cdot M_m$, or a set of sequential reversible reactions $A + M \rightleftharpoons A \cdot M$, $A + A \cdot M \rightleftharpoons A_2 \cdot M$, . . .

are assumed, the equilibrium expression will be more complex but will remain gently rounded.) If the transition represents the endpoint of the titration of AIB-binding sites, presumably in the cell membrane, by a small pool AIB contained in a discrete tissue compartment, then, because the transition does not occur in unloaded slices, this pool must be isolated from both the extracellular AIB and AIB being carried into cells. Although this pool, if it exists, must be fed by intracellular AIB, it cannot equilibrate with or even approach eqilibrium with the intracellular AIB. If it does, this small pool and the principal AIB pool will be functionally one, and any transition in a graph of P_{12} will be gradual.

If, however, the reaction between AIB and the cell membrane sites is *rate limited*, the data need not show a gradual transition, and a small pool of AIB, separate from the bulk of intracellular AIB, need not be postulated. The observed linear dependence of V'_{max} on tissue AIB in Region 1, the virtual independence of tissue AIB in Region 2, and a sharp transition are consistent with a reaction between AIB and membrane sites with a rate that is proportional to the tissue AIB and independent of the concentration of free sites, and so slow that it requires a minimum final concentration of about 19 μmol of tissue AIB/g of incubated tissue to react with all the sites within the 30-min loading period. A reaction between AIB and membrane sites will follow these kinetics if it is limited by the rate at which AIB is supplied to the sites by the slow diffusion of free cytoplasmic AIB into the membrane, or by the slow release of AIB within the membrane from one or more of the carriers for AIB efflux. If the reaction between AIB and membrane sites is limited by available AIB, it can have any stoichiometry, any mechanism, and any rate equation.

Phase Equilibria. Consider a system of three phases, in which each phase can exist over a range of concentration of a common component, X. If they are in equilibrium at a fixed temperature and pressure, the concentration of X in each phase is fixed. If one phase contains the bulk of X, this major phase dictates the overall concentration at equilibrium; any appreciable shift must cause the loss of one of the other two phases. Therefore there will be a sharp phase transition at this overall equilibrium concentration.

Let X be AIB; let the major phase be the cytoplasm, or possibly cytoplasm with organelles and the nucleus; let the two minor phases be two AIB-containing membrane phases or compartments. (The major phase cannot be the medium, because the transition process is insulated from external AIB.) Because most of the intracellular AIB is cytoplasmic, the transition between the two membrane phases must be sharp, as was observed, and therefore, except for a negligible transition range, the membrane can contain either the first phase or the second phase, but not both. The observed intersection at about 19 mol/g final wet weight of incubated tissue is compatible with a phase transition, because phase changes are not restricted by "binding sites" or

stoichiometry. If Miller's (1968) and Cabantchik and Ginsburg's (1977) data do, in fact, show breaks, their studies support a phase change, because any slow reaction between a substrate and substrate-binding sites would be complete under their equilibrium conditions.

Assume that when the membrane contains the first phase (Region 1), the carrier reverts more rapidly when loaded and therefore "exchange diffusion" occurs; and that when the membrane contains the second phase (Region 2), the rate of reversion of C_i to C_o is the same for unloaded and loaded carrier and is not affected by the AIB content of the second phase, and consequently V'_{max} is constant. If the effect of these two membrane phases on influx is different at the transition point, the transition point may not be at the intersection of the two branches of a graph of V'_{max} versus T (Fig. 2). If this is the case, then Region 1 may include the problematical data point at $S = 10\,\text{mM}$ that lies on the extrapolated curve for Region 1, and the true transition point may lie between $22.6\,\mu\text{mol/g}$ final wet weight of incubated tissue, corresponding to $S = 10\,\text{mM}$, and $25.5\,\mu\text{mol/g}$ final wet weight, corresponding to $S = 12\,\text{mM}$.

Obiter Dicta and Conclusions

Studies of phenomenological kinetics, like this one, cannot establish rate equations with complete certainty, and cannot demonstrate specific mechanisms. They can provide empirical rate equations, eliminate plausible processes that do not conform to observed rates or stoichiometries, and guide speculations about mechanisms.

The rate of AIB uptake by brain tissue containing AIB falls into one of two regions, depending on the AIB concentration in the tissue, with a sharp transition between them. Each requires its own rate equation. Two fundamentally different empirical rate equations were developed for the low-AIB region, *un embarras de richesses*. One, Eq. (5), implies that the excess influx of "exchange diffusion" is carried by transport systems for influx; the other, Eq. (14), implies that it is carried by different transport systems, probably those for efflux. Although Eq. (5) is conceptually preferable and is consistent with a carrier model for transport, Eq. (15) cannot be ruled out without further studies.

Analyses of the stoichiometry, and of the properties of binding reactions and chemical equilibria show that the transition cannot be the consequence of an equilibrum or quasi-equilibrium reaction between AIB and "AIB-binding sites" in the tissue. It may be due to an AIB-dependent phase change in cell membranes, or else to a reaction between AIB and AIB-binding sites that is first order in AIB, zero order in binding sites, and so slow that AIB in tissue must equal or exceed the transition concentration for all binding sites to react during the AIB-loading period.

Nomenclature

AIB	α-aminoisobutyric acid
A	radioactivity of reference; unspecified amino acid
C	counts in tissue sample; carrier for transport
C_i	carrier in form that reacts with intracellular substrate
C_o	carrier in form that reacts with extracellular substrate
C_R	counts in reference
CS	complex of substrate with carrier
$(CS)_i$	complex of substrate with carrier in form C_i
$(CS)_o$	complex of substrate with carrier in form C_o
G	counts per gram of tissue
HEPES	N-2-Hydroxyethylpiperazine-N'-2-ethanesulfonic acid
k_u	rate constant for first-order unsaturable uptake
K, K_α, K_β, K_σ, K_τ	adjustable parameters in Eqs. (9)–(13) for Δv, analogous to the Michaelis constant
K_d	dissociation constant
K_t	Michaelis constant for saturable uptake
K_t'	Michaelis constant for gross saturable uptake by tissue containing substrate
m_1, m_2	slope in Eq. (5) or (6) expressing dependence of $V'_{\max}$ on T or T_i^w in Region 1 or 2
M	binding site for amino acid A
n	number of data points
P	number of parameters to be determined; parameter in Stein's (1981) equation, Eq. (17) in this paper
P_1, P_2, P_{12}	property of tissue with unoccupied binding sites, property of tissue with occupied binding sites, property of tissue with both unoccupied and occupied binding sites, respectively
Q	parameter in Stein's (1981) equation, Eq. (17) in this paper
r	Pearson's correlation coefficient
Relative error RE	$= 100\{\Sigma[(\text{observed quantity} - \text{calculated quantity})/\text{calculated quantity}]^2/(n - P)\}^{1/2}$
S	concentration of substrate in medium; transport substrate
S_i	intracellular transport substrate
S_{int}	AIB in medium corresponding to intracellular AIB at intersection
S_o	extracellular transport substrate

T	observed concentration of substrate in tissue including substrate in extracellular space and adherent fluids
T_i	intracellular concentration of substrate
T_{int}	tissue AIB corresponding to intracellular AIB at intersection
T_i^w, T_i^{30}	intracellular concentration of substrate with w% (30%) extracellular and adherent fluids
U	observed uptake of labeled substrate by incubated tissue including substrate in extracellular and adherent fluids
U_R	observed uptake of labeled substrate referred to concentration of substrate in medium
$U_{\max}$	adjustable parameter in Eqs. (9)–(15) for Δv, analogous to the Michaelis–Menten maximum rate, $V_{\max}$
v	influx of substrate
v_L	gross influx of substrate into tissue containing substrate
v_L'	contribution of saturable component to gross influx into tissue containing substrate
Δv	incremental influx, that is, gross influx into tissue that contains substrate minus influx under the same conditions into tissue that does not contain substrate
V_1, V_2	intercept in Eq. (5) or (6) expressing dependence of $V'_{\max}$ on T or T_i^w in Region 1 or 2, respectively
$V_{\max}$	maximum rate in Michaelis–Menten equation
$V'_{\max}$	apparent maximum rate defined by $V'_{\max} \equiv v'_L(1 + K_t'/S)$
$V'_{\max 1}$, $V'_{\max 2}$	apparent maximum rate in Region 1 or 2, respectively
V'_{int}	apparent maximum rate at intersection defining boundary between Regions 1 and 2
w	weight of incubated tissue
W_d	dry weight of tissue expressed as fraction by weight
W_e	extracellular and "surface" space of incubated tissue expressed as percent by weight
α, β, γ	adjustable parameters in modified expressions for gross unsaturable influx into tissue containing substrate
α, β, σ, τ	exponents of S or T in Eqs. (9)–(13) for Δv
μ	parameter in Stein's (1981) equation, Eq. (17), corresponding more or less to m_1

Acknowledgments

I thank Mr. Antonio Espinal and Mr. Merrill Hessel for careful, valuable, and much appreciated technical assistance.

References

Benson, S. W. (1960). *The Foundations of Chemical Kinetics*, McGraw-Hill, New York, pp. 25, 319–414 (Chapter XIII).
Blasberg, R., and Lajtha, A. (1965). *Arch. Biochem. Biophys.* **112**, 361–377.
Cabantchik, Z. I., and Ginsburg, H. (1977). *J. Gen. Phsiol.* **69**, 75–96.
Cohen, S. R. (1968). *Analyt. Biochem.* **22**, 549–552.
Cohen, S. R. (1972). In *Research Methods in Neurochemistry* (Marks, N., and Rodnight, R., eds.), Vol. 1, Plenum Press, New York and London, pp. 179–219.
Cohen, S. R. (1973*a*). *J. Physiol. (London)* **228**, 105–113.
Cohen, S. R. (1973*b*). *Brain Res.* **52**, 309–321.
Cohen, S. R. (1974). *Exp. Brain Res.* **20**, 421–434.
Cohen, S. R. (1975). *J. Membr. Biol.* **22**, 53–72.
Cohen, S. R. (1980*a*). *J. Neurochem.* **35**, 1008–1012.
Cohen, S. R. (1980*b*). *J. Membr. Biol.* **52**, 95–105.
Cohen, S. R. (1981). *Brain Res.* **205**, 157–168.
Cohen, S. R. (1985). *J. Neurochem.* **44**, 455–464.
Cohen, S. R., Blasberg, R., Levi, G., and Lajtha, A. (1968). *J. Neurochem.* **15**, 707–720.
Cohen, S. R., Stampleman, P. F., and Lajtha, A. (1970). *Brain Res.* **10**, 419–434.
Eilam, Y., and Stein, W. D. (1974). In *Methods in Membrane Biology* (Korn, E. D., ed.), Vol. 2, Plenum Press, New York and London, pp. 283–354.
Folch-Pi, J. (1955). Cited in: Katzman, R., and Pappius, H. M. (1973). *Brain Electrolytes and Fluid Metabolism*, Williams and Wilkins, Baltimore, Table 1.4, p. 4.
Heinz, E. (1954). *J. Biol. Chem.* **211**, 781–790.
Heinz, E., and Walsh, P. M. (1958). *J. Biol. Chem.* **233**, 1488–1493.
Hoare, D. G. (1972). *J. Physiol. (London)* **221**, 311–329.
Lieb, W. R., and Stein, W. D. (1970). *Biophys. J.* **10**, 585–609.
Lieb, W. R., and Stein, W. D. (1974). *Biochim. Biophys. Acta* **373**, 178–196.
McIlwain, H., and Buddle, H. L. (1953). *Biochem. J.* **53**, 412–420.
Miller, D. M. (1968). *Biophys. J.* **8**, 1329–1338.
Stein, W. D. (1981). In *New Comprehensive Biochemistry* (Neuberger, A., and van Deenen, L. L., general eds.), Vol. 2, *Membrane Transport* (Bonting, S. L., and de Pont, J. J. H. H. M., eds.), Elsevier/North-Holland, Amsterdam, New York, and Oxford, pp. 123–157.
Ussing, H. H. (1949). *Pysiol. Rev.* **129** 127–155.
Vidaver, G. A., and Shepherd, S. L. (1969). *J. Biol. Chem.* **243**, 6140–6150.